Influence of section size on dual phase ADI microstructure and properties: comparison with fully ferritic and fully ausferritic matrices

A. Basso, R. Martínez and J. Sikora*

The present work aims to evaluate and compare the influence that section size has on the microstructure and properties of fully ferritic, fully ausferritic and dual phase ADI matrices. Samples taken from 'Y' blocks of 25, 50 and 75 mm thickness were used to perform metallographic studies and mechanical tests. Cooling rate differences arising from changes in section size promote different microsegregation characteristics affecting solid state transformations and, consequently, the final microstructure and properties.

When the section size increases, some properties decrease. The strongest deleterious effect was ascribed to the elongation and impact of ADI samples, where drops of nearly 40% were reached when specimens taken from the thinnest 'Y' blocks were compared to those taken from the thickest ones. Regarding fracture toughness, ferritic matrices exhibited the most noticeable detrimental effect. Dual phase ADI samples, on the other hand, presented the least deleterious section size effect on all the studied properties.

Keywords: Ductile iron, Dual phase ADI, Section size, Microstructures, Properties

Introduction

Ductile iron (DI) has been employed to replace cast and forged steels in a large number of applications, and its production has shown a sustained growth rate during the last decades. At present, researchers and producers continue in their search for new DI applications; the market of safety critical parts is their main target as high strength and toughness are customary requirements thereof. In this regard, austempered ductile iron (ADI) and fully ferritic DI are frequently used to such an end. A new kind of DI is currently under development; this new material is usually referred to as 'dual phase ADI' (or 'dual phase'). The matrix of this material is composed of ausferrite (regular ADI microstructure) and free (or allotriomorphic) ferrite. This combined microstructure is obtained by subjecting DI to special heat treatments comprising an incomplete austenitisation step (at temperatures within the intercritical interval) followed by an austempering step in a salt bath in order to transform the austenite into ausferrite.[1]

Up to the present, some authors have carried out research work in the field of dual phase ADI. Aranzabal *et al.*[2] have developed dual phase ADI to be used in the production of cast automotive parts, and have further reported remarkable improvements in mechanical properties. Verdu *et al.*[3] have carried out studies on fatigue properties. Kilicli *et al.*[4,5] have explored the mechanical properties for different ausferrite volume fractions and morphologies. The authors of the present paper have also started researching on this topic, analysing the effect of austempering temperature on the final microstructure and properties.[1,6]

Overall, the results of the studies predict promising applications for dual phase ADI, since this new material features very interesting mechanical and fracture toughness properties when compared to DI samples with fully ferritic or completely ausferritic matrices. In particular, significant values of the critical flaw defect, expressed by the $(K_{IC}/\sigma_{0,2})^2$ ratio, were yielded by microstructures composed of allotriomorphic ferrite containing between 20 and 40% of ausferrite.[6]

It should be highlighted at this point that all the data reported on dual phase ADI were obtained by testing samples taken from conventional 'Y' blocks of 25 mm thickness. Nonetheless, it is common knowledge that the mechanical properties of cast iron parts are closely related to solidification microstructure, which, in turn, is influenced by the size of the cast part.[7,8] Then, the industrial parts to be manufactured using dual phase ADI should be designed considering size effects.

Ductile irons are complex alloys containing several chemical elements such as Mn, Si, Mg, S and P, while other elements such as Mo, Cu and Ni are frequently used as alloy elements. Owing to the microsegregation phenomena that take place during solidification, the metallic matrix of cast iron does not display a homogeneous chemical composition. Chemical elements such

Faculty of Engineering, INTEMA, Universidad Nacional de Mar del Plata, CONICET Av. Juan B. Justo 4302 (B7608FDQ), Mar del Plata, Argentina

*Corresponding author, e-mail jsikora@fi.mdp.edu.ar

Published by Maney on behalf of the Institute
Received 29 May 2008; accepted 17 July 2008
DOI 10.1179/174328408X365784

as Mn, Mo, Cr, P, etc. exhibit a direct segregation tendency, while Si, Ni and Cu show an inverse segregation trend.[7,8] The characteristics of the last to freeze zones (LTF) play a significant role when high performance DI parts are required. Their adverse tensile properties result from the microstructural heterogeneity produced by microsegregation as well as the fact that most cast defects, such as pores, microvoids, inclusions, etc., are detected in these regions' account.[7]

The mounting interest in the industrial applications of high strength DI parts has led the authors to study the influence of section size on the final microstructure and mechanical properties of dual phase ADI, and to compare this effect to fully ferritic and fully ausferritic matrices.

Experimental methods

Material and samples

A ductile iron melt was prepared in a medium frequency induction furnace at an industrial foundry plant (MEGAFUND SA). Steel scraps and foundry returns were used as raw materials. The nodularisation step was conducted using the sandwich method, employing 1·5 wt-% of Fe–Si–Mg (6%Mg). The melt was inoculated with 0·6 wt-% Fe–Si (75%Si). Approximately 0·9%Cu was added in order to improve austemperability.

The melt was poured in 'Y' block shaped sand moulds of 25, 50 and 75 mm thickness. Round (12 mm diameter and 100 mm length) and prismatic ($15 \times 25 \times 105$ mm) samples were cut from the Y blocks and used to prepare specimens for metallographic studies, and to conduct tensile and fracture toughness tests.

Heat treatments

All the samples employed in the present work were previously ferritised following an annealing heat treatment cycle consisting of

(i) austenitising at 900°C for 3 h
(ii) cooling down to 740°C inside the furnace
(iii) holding at 740°C for 10 h
(iv) cooling down to room temperature inside the furnace.

The methodology employed to establish the intercritical interval for a specific alloy has been detailed in previous works,[1,6] and is herein summarised as follows: several ferritised specimens of 12 mm in diameter and 25 mm in length were subjected to thermal cycles involving austenitising stages ranging from 730 to 900°C at steps of 10°C. Each complete thermal cycle consisted of holding the sample for 1 h in the furnace at a selected austenitising temperature ($T\gamma$). After the heating step, the samples were water quenched. The resulting microstructures were composed of different amounts of ferrite (original matrix) and martensite (quenched austenite).

The heat treatment cycle used to obtain dual phase ADI samples comprised a first step wherein partial austenitisation was obtained by holding the samples in the furnace within the intercritical interval at 810°C for 1 h, followed by an austempering step at 350°C for 90 min. These heat treatment variables were selected to produce a microstructure composed of about 30–40% ausferrite and 60–70% free ferrite in view of previous works which had demonstrated that such microstructures yielded interesting mechanical properties and fracture toughness.[6]

Samples with fully ferritic (ferritised) and fully ausferritic (conventional ADI) matrices were also used in the present work to compare the effects of section size on three different microstructures.

Conventional ADI samples were obtained by performing a heat treatment cycle consisting of a complete austenitising step at 910°C for 1 h, followed by austempering at 350°C for 90 min.

The ferritising treatments as well as all the austenitising steps were carried out in electric furnaces, while a 500 kg salt bath was used to perform the austempering steps.

The microconstituents were quantified using an optical microscope and Image Pro Plus software. Reported values are the average of at least three determinations. The percentages of the reported phases did not include the graphite areas.

Mechanical tests

Tensile tests were carried out in accordance with ASTM E8M/88 standard, using a universal testing machine (INSTRON 8501).

Unnotched Charpy samples of $10 \times 10 \times 55$ mm were tested in compliance with the ASTM E23 standard, using an impact machine which delivered an impact speed of 5 m s^{-1}. The fracture toughness parameter K_{IC} was determined using SEN (B) standard specimens of $10 \times 20 \times 100$ mm, following the specifications given by the ASTM E399 standard. The test specimens were premachined, heat treated, machined to final dimensions, notched, precracked and tested. The notches were machined with an electro-erosion machine, and precracking was conducted applying a cyclic load with a double eccentric machine. The final crack length was measured using a profile projector. The values of the properties reported are the average of testing at least three samples.

Results and discussion

As cast microstructures

The melt chemical composition is listed in Table 1. The as cast microstructure was pearlitic-ferritic, and the nodularity range exceeded 90%, according to ASTM A-247 standard.

Nodule counts of 200, 110 and 50 nodules mm^{-2} were measured on samples taken from the 25, 50 and 75 mm 'Y' blocks respectively. After the ferritising treatment, the matrix of all samples became fully ferritic. Figure 1 shows representative microstructures of samples taken from the three different 'Y' block sizes.

Intercritical interval

The intercritical interval was determined in accordance with the procedure described in the section on 'Material and samples', using only samples taken from 25 mm 'Y' blocks.

Table 1 Chemical composition (wt-%)

C	Si	Mn	Cu	Mg	S, P	CE
3·35	3·21	0·46	0·94	0·042	< 0·02	4·26

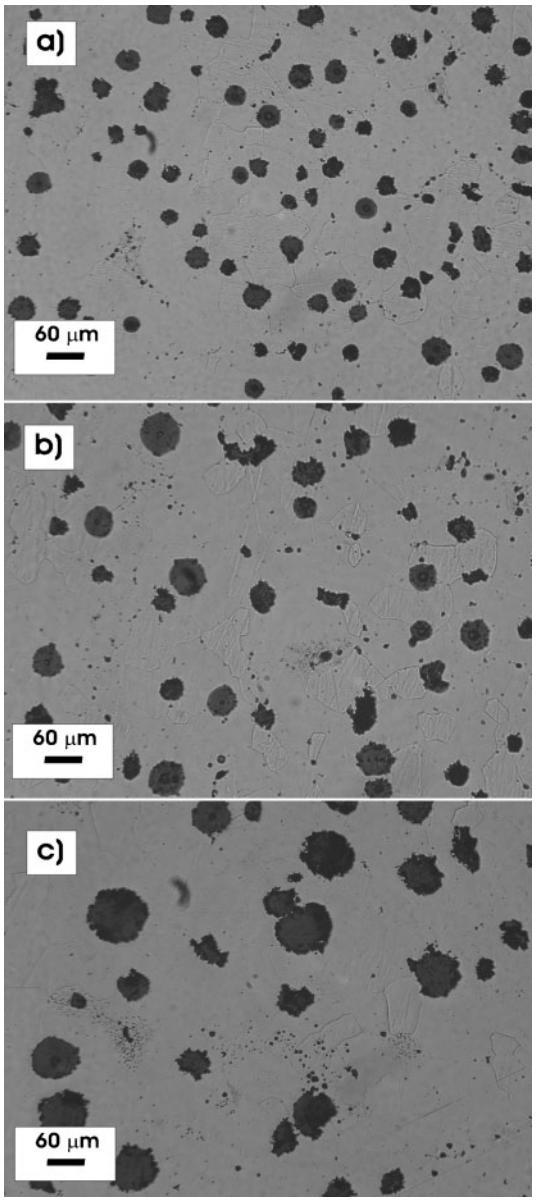

a 25 mm; *b* 50 mm; *c* 75 mm

1 Entirely ferritic microstructures of samples taken from 'Y' blocks

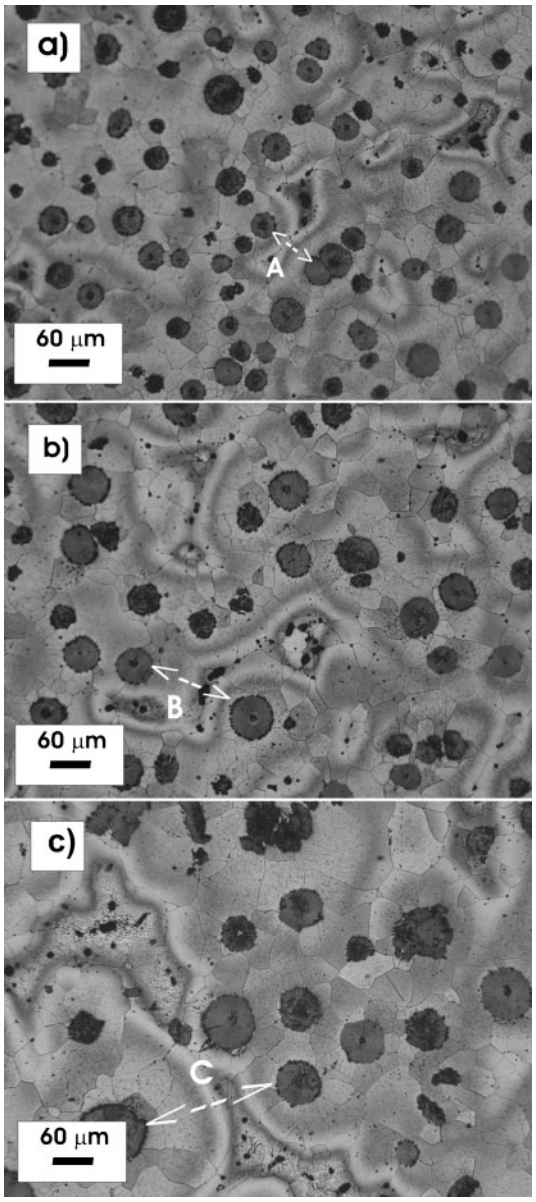

a 25 mm; *b* 50 mm; *c* 75 mm

2 Black and white prints of colour etching micrographs of fully ferritic matrices for samples taken from 'Y' blocks of different thicknesses

The lower critical temperature (L_{ct}) was defined as 770°C, since the ferrite into austenite transformation (martensite after quenching) started at such a temperature. The upper critical temperature (U_{ct}), in turn, was fixed at 860°C, having obtained a matrix with over 98% of martensite from samples quenched from such a temperature.

Influence of section size on phase transformations taking place within intercritical interval

Figure 2*a*–c is black and white prints of colour micrographs corresponding to fully ferritic matrices of samples taken from the 25, 50 and 75 mm 'Y' blocks. They were obtained using a special colour etching technique developed by Rivera *et al.*,[7] which enables the visualisation of the shape, size and distribution of LTF zones in the microstructure.

It can be observed that when the cast section size increases, the resulting LTF zones become larger (*see* the areas in the middle of the arrows referred to as A, B and C in Fig. 2*a*–c)

In order to analyse the effect that the section size has on the intercritical interval range, two sets of samples were heated in an electric furnace. Each set was made up of samples taken from 'Y' blocks of 25 and 75 mm. They were held at different temperatures for 1 h, and then water quenched so as to evaluate transformation differences. The selected temperatures were 760 and 800°C. Note that 770°C is the lower critical temperature determined on samples taken from 25 mm 'Y' blocks, while 800°C is an intermediate temperature within the intercritical interval. Figure 3 shows the microstructures obtained after heat treatment. With regard to the sample corresponding to the 25 mm 'Y' block, held at 760°C, no martensite areas were observed (*see* Fig. 3*a*). This means that, for this sample, heat treatment had been effectively conducted below the lower critical temperature with no

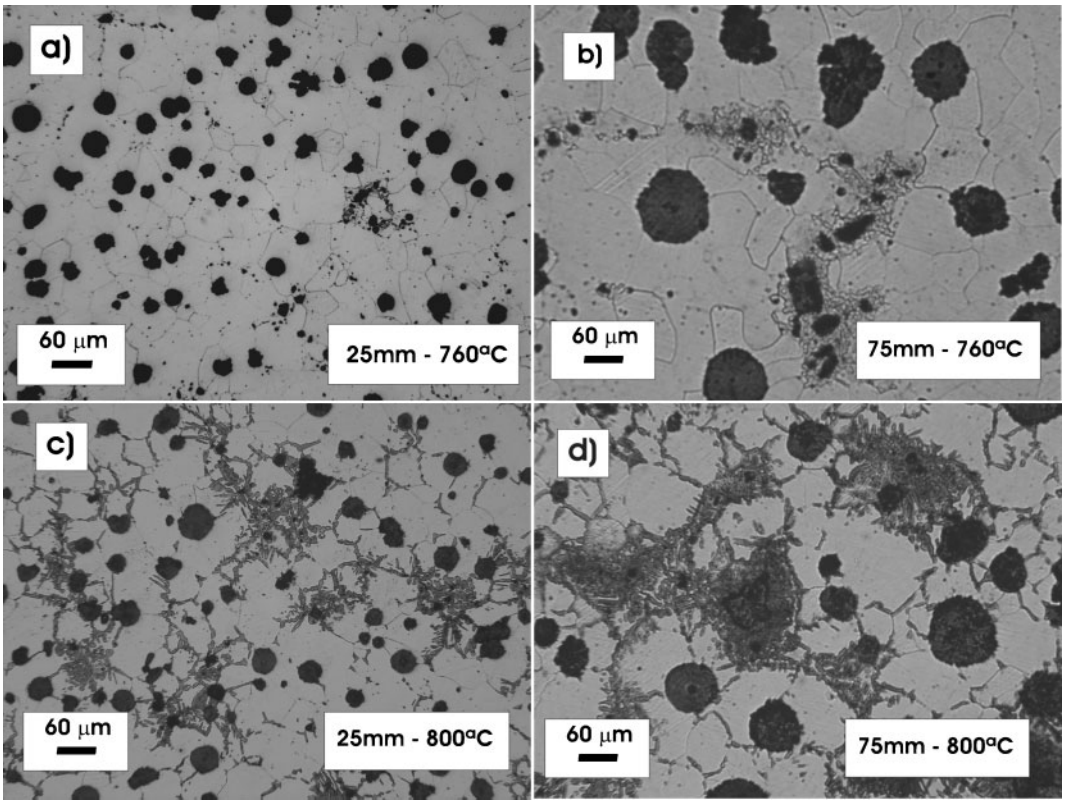

3 Effect of section size on solid phase transformations in intercritical interval

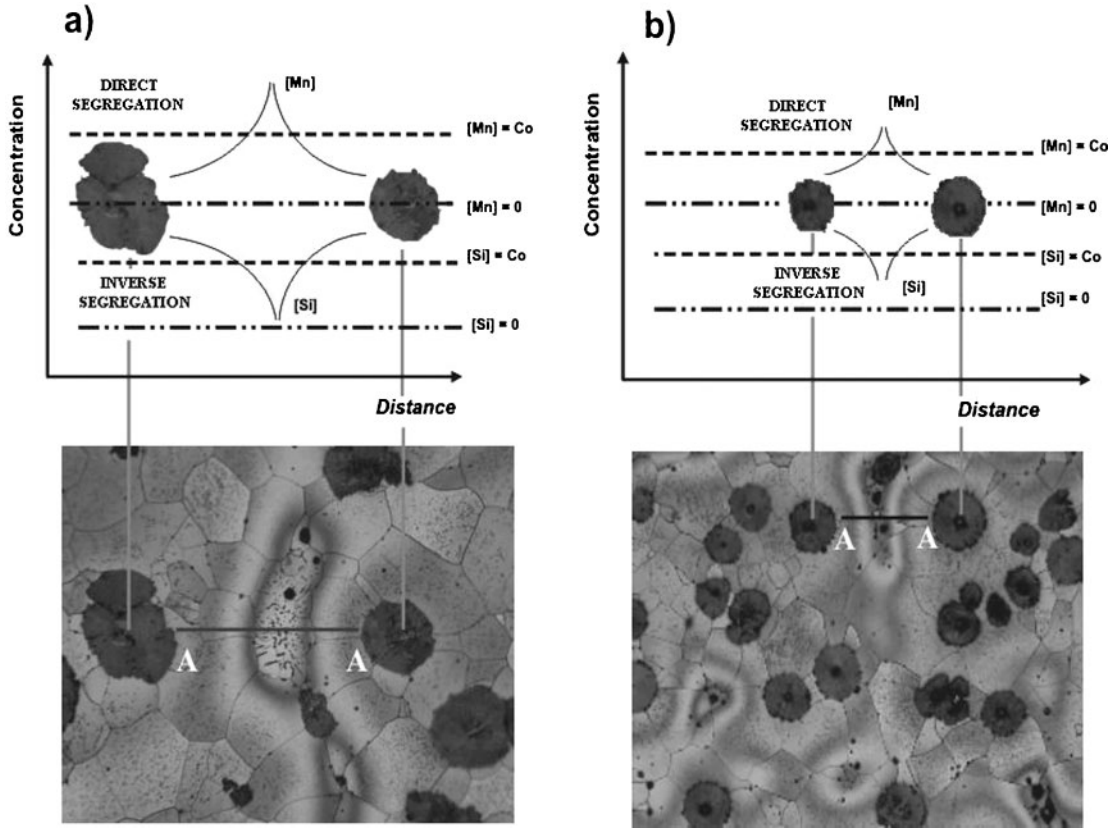

a 75 mm; *b* 25 mm

4 Black and white prints of colour micrographs and qualitative plots of Mn and Si distribution profiles for samples of different thickness

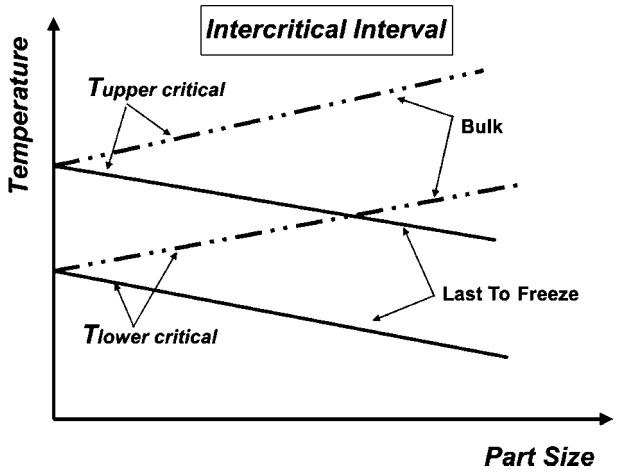

5 Scheme of section size effect on critical temperatures at bulk and LTF zones

ferrite into austenite transformation. However, for the sample from the 75 mm 'Y' block held in the furnace at the same temperature (760°C), several martensite areas can be observed (Fig. 3*b*), coinciding with the LTF zone locations. The presence of martensite is attributed to the lower critical temperature of these zones, due to the higher contents of alloying elements with direct segregation tendencies (such as Mn).

Figure 3*c* and *d* depicts the microstructures corresponding to the set of samples held at 800°C. Figure 3*d* clearly shows larger amounts of martensite in comparison with Fig. 3*c*. Again, differences are ascribed to the effect of the solidification rate on microsegregation and consequently on solid state transformations. As stated in previous works,[1,6] austenite nucleation and growth within the intercritical interval start in LTF zones, where the lower critical temperature is decreased by the higher level of alloying elements (such as Mn), thereby favouring the ferrite to austenite transformation. On the other hand, the larger amount of Si present in the bulk increases the upper critical temperature in these zones.

To summarise this concept and take into account Scheil's prediction as well as actual measurements made on different DI samples,[9–12] Fig. 4 sketches a qualitative variation of solute concentration in the metallic matrix as a function of the solidification distance. Figure 4 shows the effect that the section thickness has on the distribution profiles of two typical chemical elements, Mn and Si, displaying direct and inverse microsegregation tendencies respectively. To simplify this scheme, it is considered that solidification advances between two graphite nodules chosen following the A–A lines (Fig. 4). Figure 4*b* illustrates the possible chemical composition differences on the A–A line for the sample taken from a 25 mm 'Y' block, where the microsegregation pattern is revealed by colour etching in the micrograph below. On the other hand, Fig. 4*a* presents a similar case but for a 75mm 'Y' block sample, where the LTF zones clearly exhibit coarser features (larger A–A distance) and higher concentration peaks.

Taking into account the shape of the microsegregation profiles, the role played by section size (solidification rate) on the intercritical interval can be understood in view of the upper and lower critical temperatures, and hence the intercritical interval amplitude is modified by

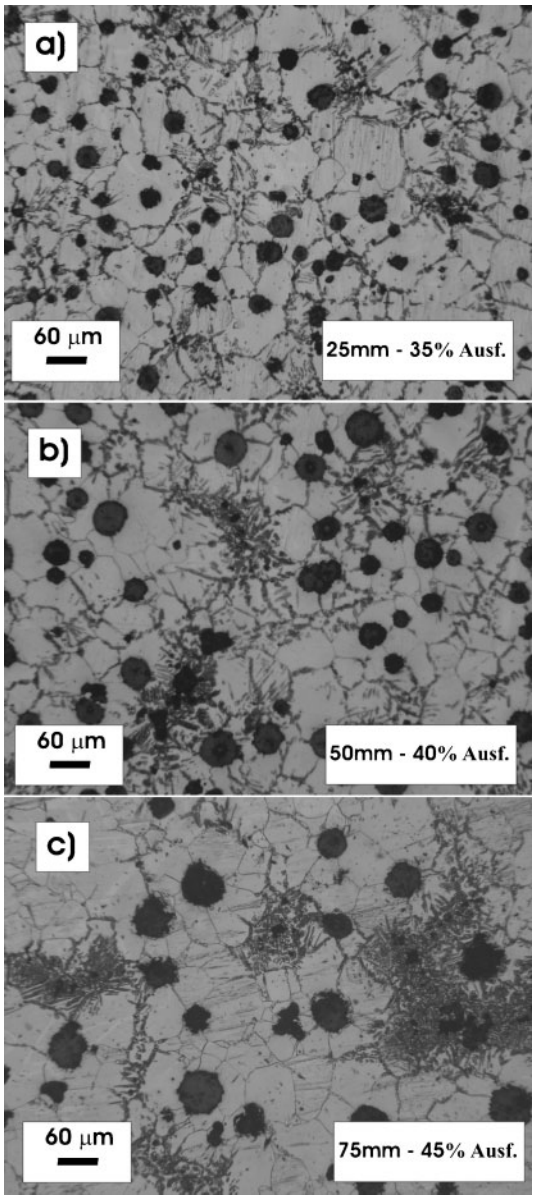

6 Micrographs of dual phase ADI in samples taken from different section size

the alloy heterogeneous chemical composition. In fact, the literature reports several equations for the determination of the upper critical temperature in relation to the influence of some of the most common alloying elements.[13] As an example, the equation developed by Sikora *et al.*[14] establishes that

$$U_{ct} = 723 - 0{,}3\%C + 43\%Si - 33\%Mn - 6\%Cu \qquad (1)$$

It is worth mentioning that this kind of equations has always been developed assuming a homogeneous distribution of the alloying elements. Besides, they were determined from experimental data obtained from samples taken from conventional 25 mm 'Y' blocks cast in sand moulds, where a constant cooling rate can be presupposed. To the best of the authors' knowledge, no equation determining the lower critical temperature has been reported.

To put it in a few words, for samples of a same melt, the upper and lower critical temperatures are expected to

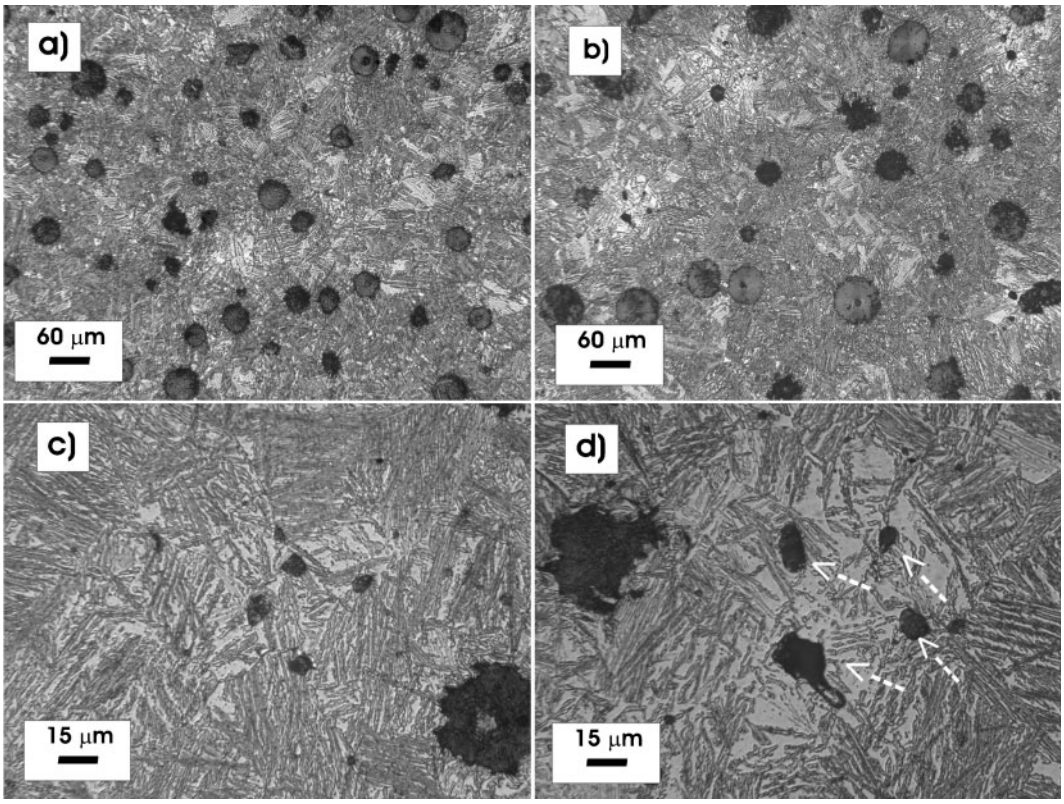

a and *c* 25 mm; *b* and *d* 75 mm

7 Ausferritic matrices for samples taken from sections of different size

move up and down respectively, depending on the characteristics of the microsegregation phenomena, which, in turn, are governed by the cooling rate imposed by the piece size. Therefore, changes in solid state transformations are expected to take place. Figure 5 qualitatively sketches the effect of the solidification rate (represented by the 'Y' block size) on the critical temperatures in the bulk as well as in LTF zones.

Influence of section size on final microstructure

Figure 6 shows dual phase microstructures corresponding to samples taken from 'Y' blocks of the three thicknesses studied. All samples have been heat treated simultaneously using the thermal cycle described in the section on 'Heat treatments', which consists in holding the samples at 810°C for 1 h, followed by austempering at 350°C for 90 min. Figure 6a–c shows that the thicker the 'Y' block, the greater the amount of ausferrite present in the matrix.

Figure 7 illustrates the microstructures corresponding to samples with fully ausferritic matrices (completely austenitised at 910°C) with different magnifications obtained from samples taken from 'Y' blocks of 25 mm (Fig. 7*a* and *c*) and 75 mm (Fig. 7*b* and *d*). The increasing amount of unreacted austenite in the LTF zones (lighter areas in the pictures) can be seen in samples taken from the 75 mm 'Y' block (Fig. 7*d*) in comparison with those of the 25 mm 'Y' block (Fig. 7*c*). Concurrently, a higher concentration of casting defects, such as non-metallic inclusions (pointed by the arrows in Fig. 7*d*) are present in all cases in the largest LTF areas corresponding to the thickest parts.

Influence of section size on mechanical properties

Figure 8 displays tensile properties as a function of section size for the three types of microstructures studied in the present work, while Fig. 9 shows the results of impact tests (Charpy). When the section size increases, tensile strength and elongation decrease for samples with ausferritic matrices, while the yield stress remains unchanged. On the other hand, impact properties decrease for all matrices. This behaviour is attributed to the fact that fracture mechanisms, involving microvoid nucleation and coalescence, generally arise from defects such as inclusions and pores located in LTF zones.[8] Then, if the size of LTF areas increases so does the deleterious effect on mechanical properties.

For a more accurate analysis of the influence that section size exerts on mechanical properties, Fig. 10 shows the drops in tensile strength, elongation and impact (in percentages) corresponding to samples machined from 25 mm 'Y' blocks in relation to those taken from 75 mm 'Y' blocks, for the three matrices studied.

The results reproduced in Fig. 10 lead to the conclusion that the increase in section size had a stronger effect in ADI samples. This effect is more noticeable in elongation and impact resistance, where drops of over 40% were reached.

Figure 11*a* shows the section size effect on K_{IC} values for the different matrices. Ferritic samples show larger variations if compared to fully ausferritic and dual phase matrices.

Figure 11*b* shows the results of the section size effect on the $(K_{IC}/\sigma_{0,2})^2$ ratio. Significant variations were detected again for ferritic matrices. It is worth noting

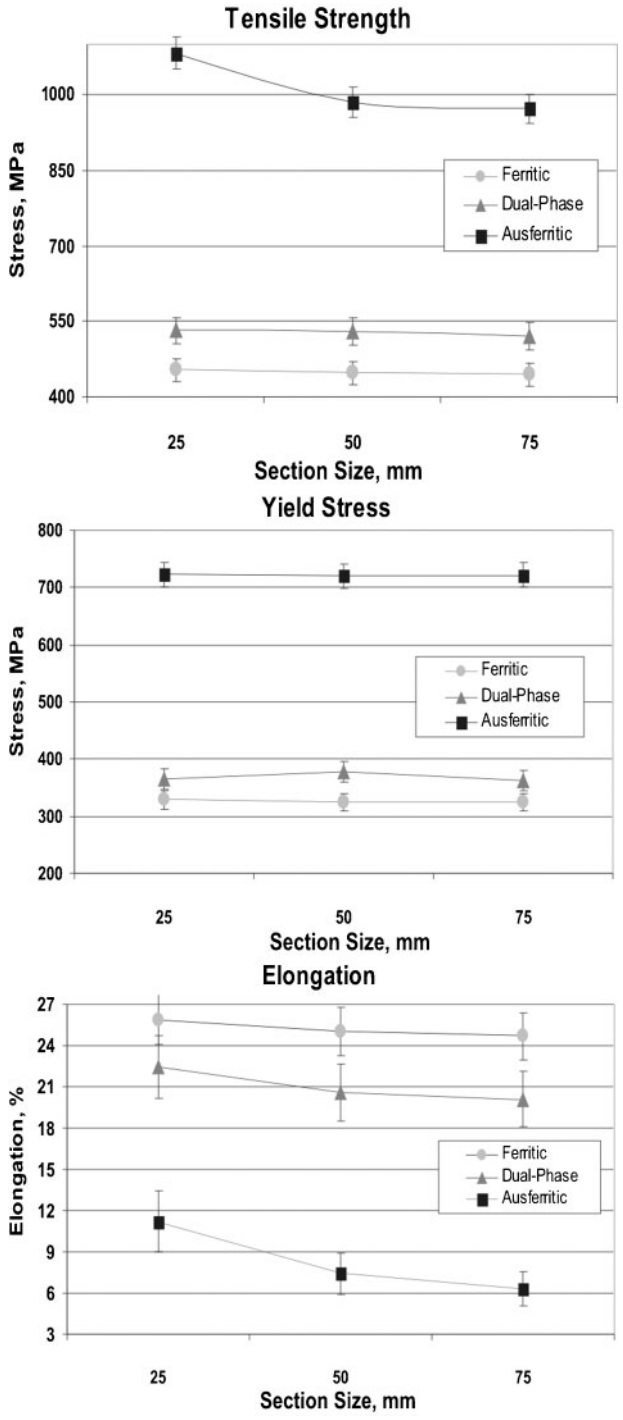

8 Tensile properties for different section sizes and matrix microstructures

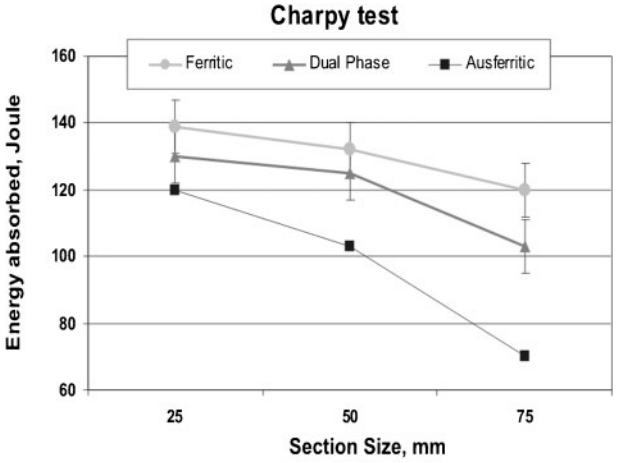

9 Impact properties for different section sizes and matrix microstructures

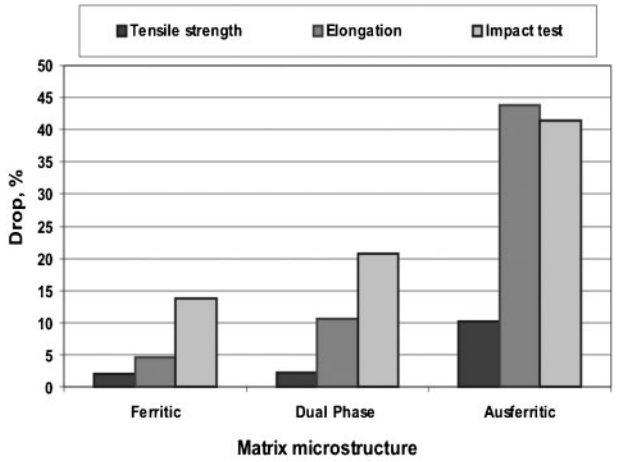

10 Drops (%) in tensile and impact properties between samples obtained from 'Y' blocks of 25 and 75 mm

that in the design and manufacture of mechanical components, the parts are expected to be able to tolerate yield stress loading in tension without failing in local regions, and that the yield stress loading may occur in the vicinity of structural discontinuities. Then, the critical crack size is often proportional to $(K_{IC}/\sigma_{0,2})^2$, which becomes a proper index to measure the material relative toughness, considering that the ability to tolerate large flaws without fracture is always desirable. In other words, the use of materials with a $K_{IC}/\sigma_{0,2}$ ratio as high as possible should be pursued.

Figure 12 displays the variation percentages of the fracture properties for the three microstructures studied. The results show that dual phase microstructures are the least sensitive to the deleterious effect that the increase of section size has on mechanical properties and fracture toughness.

Conclusions

1. Differences in the cooling rate due to changes in section size give rise to different LTF zone characteristics in all DI castings, affecting the final microstructure and properties. As a general rule, the greater the section size, the larger the LTF areas.

2. Regarding the austenitising step, austenite nucleation and growth at temperatures within the intercritical interval starts in LTF zones, because of the higher levels of alloying elements (e.g. Mn). As a consequence, the lower critical temperature diminishes and the ferrite into austenite transformation is favoured.

3. The influence of section size on the final microstructure and mechanical properties of dual phase ADI has been compared to fully ferritic and fully ausferritic matrices.

4. Increasing section size leads to greater effects on the elongation and impact properties of ADI, where drops

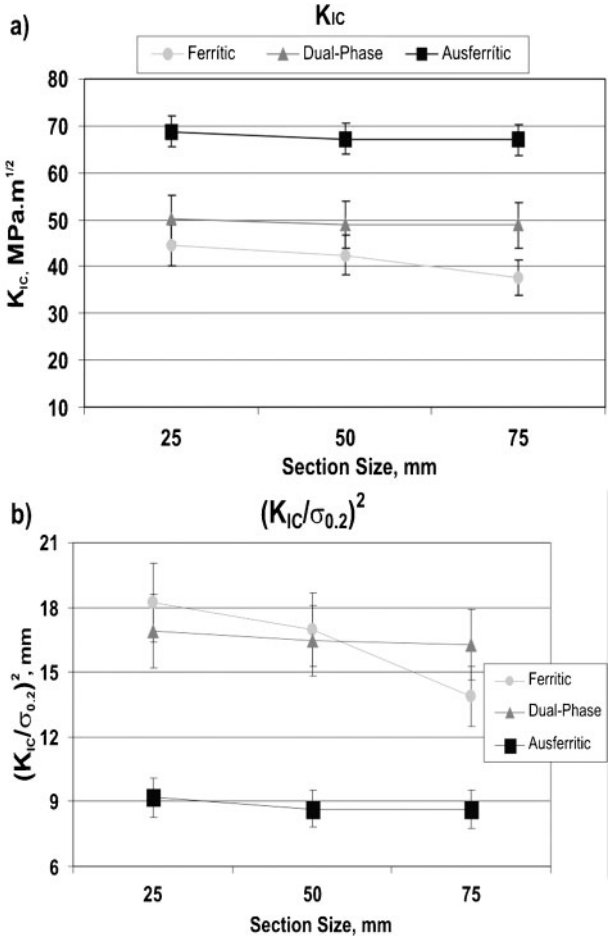

a K_{IC}; *b* $(K_{IC}/\sigma_{0,2})^2$

11 Fracture toughness properties for different section sizes and different matrices

of nearly 40% were reached when samples taken from 25 mm were compared to those taken from 75 mm 'Y' blocks.

5. With regard to fracture toughness properties, the most noticeable deleterious effect of increasing section size has been detected in ferritic matrices.

6. Dual phase ADI microstructures are the least sensitive to the deleterious effect of section size increment on mechanical properties and fracture toughness.

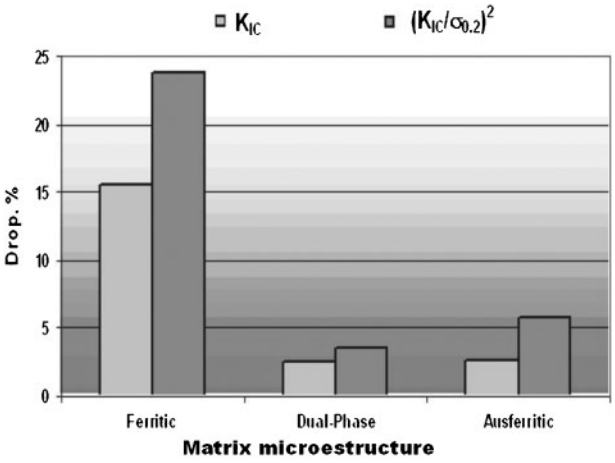

12 Drops (%) in fracture toughness and critical flaw defect between samples obtained from 'Y' blocks of 25 and 75 mm

Acknowledgements

The financial support granted by CONICET, SECYT and the Universidad Nacional de Mar del Plata is gratefully acknowledged.

References

1. A. Basso, R. A. Martínez and J.A. Sikora. Proc. 8th Int. Symp. on 'Science and processing of cast iron', Beijing, China, October 2006, Tsinghua University, 408–413.
2. J. Aranzabal, G. Serramoglia, C.A. Goria and D. Rousiere: *Int. J. Cast Met. Res.*, 2002, **16**, (1), 185–190.
3. C. Verdu, J. Adrien and A. Reynaud: *Int. J. Cast Met. Res.*, 2005, **18**, (6), 346–354.
4. V. Kilicli and M. Erdogan: *Mater. Sci. Technol.*, 2006, **22**, (8), 919–928.
5. V. Kilicli and M. Erdogan: *Int. J. Cast Met.*, 2007, **20**, (4), 202–214.
6. A. Basso, R. A. Martínez and J. A. Sikora: *Mater. Sci. Technol.*, 2007, **23**, (11), 1321–1326.
7. G. Rivera, R. Boeri and J. Sikora: *Mater. Sci. Technol.*, 2002, **18**, (6), 691–697.
8. G. Rivera, R. Boeri and J. Sikora: *Int. J. Cast Met. Res.*, 1999, **11**, 533–538.
9. R. Boeri and F. Weingberg: *Int. J. Cast. Met.*, 1993, **6**, 153–158.
10. G. Rivera, R. Boeri and J. Sikora: Int. *J. Cast Met.*, 1995, **8**, (1), 1–5.
11. A. Giacopini, R. Boeri and J. Sikora: *Mater. Sci. Technol.*, 2003, **19**, (12), 1755–1760.
12. S. I. Karsay: 'Ductile iron: state of the art'; Quebec Iron and Titanium Corp, Quebec, Canada, 1976.
13. H. T. Angus: 'Cast iron: phyical and enginnering properties', 2nd edn; 1976, London, Butterworths.
14. I. Galarreta, R. Boeri and J. Sikora: *Int. J. Cast Met. Res.*, 1997, **9**, (6), 353–358.